

All-sky search for gravitational waves

Andrzej Królak^{1,2} and Pia Astone³

¹*Jet Propulsion Laboratory, USA.*

²*permanent address: Institute of Mathematics,
Polish Academy of Sciences, Poland.*

³*Istituto Nazionale di Fisica Nucleare, (INFN)-Rome I, 00185 Rome, Italy*

We present first results of the all-sky search for gravitational wave signals from spinning neutron stars in the data of the EXPLORER bar detector. Our data analysis technique is based on the maximum likelihood detection method that is related to the matched-filtering technique. This method is optimal in the sense that it maximizes the probability of detection of the signal. We give an outline of the theoretical methods that we used in the search. We show that if our search will not reveal a gravitational wave signal we shall still be able to impose a useful upper bound of 2×10^{-23} for the dimensionless amplitude of such a signal.

1 Introduction

It is a unique property of the gravitational-wave detectors that with a single time series one can search for signals coming from all sky directions. In the case of other instruments like optical and radio telescopes to cover the whole or even part of the sky requires a large amount of expensive telescope time. However the gravitational wave signals are very weak and are deeply buried in the noise of the detector. Consequently the detection of these signals and interpretation of data analysis results is a very difficult task. From this point of view one type of sources is very attractive. These are continuous sources like for example spinning neutron stars. A signal from such a source has definite characteristics that make it suitable for application of the optimal detection techniques based on matched filtering. Moreover such signals are stable and will always be present in the data. This enables reliable verification of the potential candidates by repeating the observations both by the same detector and by other detectors. For these reasons we considered the all-sky search for continuous sources as our first task in the analysis of the gravitational-wave data.

The directed search of the galactic center has already been carried out and limits for the amplitude of the gravitational waves has been established [3].

Our paper is divided into two parts. In the first part we shall review the theoretical tools that we used in our analysis and in the second part we shall present first

results of our all-sky search. Some more details of the search can be found on our website: <http://www.astro.uni.torun.pl/~kb/AllSky/AllSky.html>.

The data analysis was performed by a team consisting of Pia Astone, Kaz Borkowski, Piotr Jaranowski and Andrzej Królak and was carried out on the basis of Memorandum of Understanding between the ROG collaboration and Institute of Mathematics of Polish Academy of Sciences.

2 Tools for data analysis

2.1 Response of the bar detector to a continuous gravitational-wave signal

2.1.1 The exact model

Dimensionless noise-free response function h of a resonant bar gravitational-wave detector to a weak plane gravitational wave in the long wavelength approximation [i.e. when the size of the detector is much smaller than the reduced wavelength $\lambda/(2\pi)$ of the wave] can be written as a linear combination of the *wave polarization functions* h_+ and h_\times :

$$h(t) = F_+(t) h_+(t) + F_\times(t) h_\times(t), \quad (1)$$

where F_+ and F_\times are called the *beam-pattern functions*. The functions read

$$\begin{aligned} F_+(t) &= a(t) \cos 2\psi + b(t) \sin 2\psi, \\ F_\times(t) &= b(t) \cos 2\psi - a(t) \sin 2\psi, \end{aligned} \quad (2)$$

where ψ is the polarization angle of the wave and

$$\begin{aligned} a(t) &= \frac{1}{2}(\cos^2 \gamma - \sin^2 \gamma \sin^2 \phi)(1 + \sin^2 \delta) \cos[2(\alpha - \phi_r - \Omega_r t)] \\ &\quad + \frac{1}{2} \sin 2\gamma \sin \phi (1 + \sin^2 \delta) \sin[2(\alpha - \phi_r - \Omega_r t)] \\ &\quad - \frac{1}{2} \sin^2 \gamma \sin 2\phi \sin 2\delta \cos[\alpha - \phi_r - \Omega_r t] \\ &\quad + \frac{1}{2} \sin 2\gamma \cos \phi \sin 2\delta \sin(\alpha - \phi_r - \Omega_r t) \\ &\quad + \frac{1}{2}(1 - 3 \sin^2 \gamma \cos^2 \phi) \cos^2 \delta, \\ b(t) &= -\sin 2\gamma \sin \phi \sin \delta \cos[2(\alpha - \phi_r - \Omega_r t)] \end{aligned}$$

$$\begin{aligned}
& +(\cos^2 \gamma - \sin^2 \gamma \sin^2 \phi) \sin \delta \sin[2(\alpha - \phi_r - \Omega_r t)] \\
& - \sin 2\gamma \cos \phi \cos \delta \cos(\alpha - \phi_r - \Omega_r t) \\
& - \sin^2 \gamma \sin 2\phi \cos \delta \sin(\alpha - \phi_r - \Omega_r t).
\end{aligned} \tag{3}$$

In Eqs. (2) and (3) the angles α and δ are respectively right ascension and declination of the gravitational-wave source. The geodetic latitude of the detector's site is denoted by ϕ , the angle γ determines the orientation of the bar detector with respect to local geographical directions: γ is measured counter-clockwise from East to the bar's axis of symmetry. The rotational angular velocity of the Earth is denoted by Ω_r , and ϕ_r is a deterministic phase which defines the position of the Earth in its diurnal motion at $t = 0$ (the sum $\phi_r + \Omega_r t$ essentially coincides with the local sidereal time of the detector's site, i.e. with the angle between the local meridian and the vernal point).

We are interested in a continuous gravitational wave, which is described by the wave polarization functions of the form

$$h_+(t) = h_{0+} \cos \Psi(t), \tag{4}$$

$$h_\times(t) = h_{0\times} \sin \Psi(t), \tag{5}$$

where h_{0+} and $h_{0\times}$ are independent amplitudes of the two wave polarizations. These amplitudes depend on the physical mechanisms generating the gravitational wave. In the case of a wave originating from a spinning neutron star these amplitudes can be estimated by

$$h_o = 4.23 \times 10^{-23} \left(\frac{\epsilon}{10^{-5}} \right) \left(\frac{I}{10^{45} \text{ g cm}^2} \right) \left(\frac{1 \text{ kpc}}{r} \right) \left(\frac{f}{1 \text{ kHz}} \right)^2, \tag{6}$$

where I is the neutron star moment of inertia with respect to the rotation axis, ϵ is the poloidal ellipticity of the star, and r is the distance to the star. The value of 10^{-5} of the parameter ϵ in the above estimate should be treated as an upper bound. In reality it may be several orders of magnitude less. The phase Ψ of the wave is given by

$$\Psi(t) = \Phi_0 + \Phi(t), \tag{7}$$

$$\Phi(t) = \sum_{k=0}^{s_1} \omega_k \frac{t^{k+1}}{(k+1)!} + \frac{\mathbf{n}_0 \cdot \mathbf{r}_{\text{SSB}}(t)}{c} \sum_{k=0}^{s_2} \omega_k \frac{t^k}{k!}. \tag{8}$$

In Eqs. (7) Φ_0 is the initial phase of the wave form, \mathbf{r}_{SSB} is the vector joining the solar system barycenter (SSB) with the detector, \mathbf{n}_0 is the constant unit vector in the direction from the SSB to the neutron star. We assume that the gravitational wave form is

almost monochromatic around some angular frequency ω_0 which we define as instantaneous angular frequency evaluated at the SSB at $t = 0$, ω_k ($k = 1, 2, \dots$) is the k th time derivative of the instantaneous angular frequency at the SSB evaluated at $t = 0$. To obtain formulas (7) we model the frequency of the signal in the rest frame of the neutron star by a Taylor series. For the detailed derivation of the phase model (7) see Sec. II B and Appendix A of Ref. [1]. The integers s_1 and s_2 are the number of spin downs to be included in the two components of the phase. We need to include enough spin downs so that we have a sufficiently accurate model of the signal to extract it from the noise. The vector \mathbf{r}_{SSB} is the sum of two vectors: the vector \mathbf{r}_{ES} joining the solar system barycenter and the Earth barycenter and vector \mathbf{r}_{E} joining the Earth barycenter and the detector. The vector \mathbf{r}_{ES} can be obtained from the JPL Planetary and Lunar Ephemerides: “DE405/LE405”. They are available via the Internet at anonymous ftp: `navigator.jpl.nasa.gov`, the directory: `ephem/export`. Whereas the vector \mathbf{r}_{E} can be accurately computed using the International Earth Rotation Service (IERS) tables available at `http://hpiers.obspm.fr/iers/eop/eopc04`. The codes to read the above files and to calculate vector \mathbf{r}_{SSB} were developed by Kazik Borkowski and they are described in Ref. [4].

It is convenient to write the response of the gravitational-wave detector given above in the following form

$$h(t) = \sum_{i=1}^4 A_i h_i(t), \quad (9)$$

where the four constant amplitudes A_i are given by

$$A_1 = (h_{0+} \cos 2\psi \cos \Phi_0 - h_{0\times} \sin 2\psi \sin \Phi_0), \quad (10)$$

$$A_2 = (h_{0\times} \cos 2\psi \sin \Phi_0 + h_{0+} \sin 2\psi \cos \Phi_0), \quad (11)$$

$$A_3 = (-h_{0+} \cos 2\psi \sin \Phi_0 - h_{0\times} \sin 2\psi \cos \Phi_0), \quad (12)$$

$$A_4 = (h_{0\times} \cos 2\psi \cos \Phi_0 - h_{0+} \sin 2\psi \sin \Phi_0). \quad (13)$$

The time dependent functions h_i have the form

$$\begin{aligned} h_1(t) &= a(t) \cos \Phi(t), \\ h_2(t) &= b(t) \cos \Phi(t), \\ h_3(t) &= a(t) \sin \Phi(t), \\ h_4(t) &= b(t) \sin \Phi(t), \end{aligned} \quad (14)$$

where the functions a and b are given by Eqs. (3), and Φ is the phase given by Eq. (8). The modulation amplitudes a and b depend on the right ascension α and the

declination δ of the source (they also depend on the angles ϕ and γ). The phase Φ depends on the frequency ω_0 , s spin-down parameters ω_k ($k = 1, \dots, s$), and on the angles α , δ . We call parameters ω_0 , ω_k , α , δ the *phase parameters*. Moreover the phase Φ depends on the latitude ϕ of the detector. The whole signal h depends on $s + 5$ unknown parameters: h_{0+} , $h_{0\times}$, α , δ , ω_0 , ω_k .

2.1.2 An approximate model

The phase of the gravitational-wave signal contains terms arising from the motion of the detector with respect to the SSB. These terms consist of two contributions, one which comes from the motion of the Earth barycenter with respect to the SSB, and the other which is due to the diurnal motion of the detector with respect to the Earth barycenter. The first contribution has a period of one year and thus for shorter observation times can be well approximated by a few terms of the Taylor expansion. The second term has a period of 1 sidereal day and to a very good accuracy can be approximated by a circular motion. We find that for two days of observation time that we used in the analysis of the EXPLORER data presented in the next section we can truncate the expansion at terms that are quadratic in time. Moreover in the Taylor expansion of the frequency parameter it is sufficient to include terms up to the first spin down. We thus propose the following *approximate* simple model of the phase of the gravitational-wave signal:

$$\Psi_s(t) = p + p_0 t + p_1 t^2 + A \cos(\Omega_r t) + B \sin(\Omega_r t), \quad (15)$$

where Ω_r is the rotational angular velocity of the Earth. The parameters A and B can be related to the right ascension α and the declination δ of the gravitational-wave source through the equations

$$A = \frac{\omega_0 r_E}{c} \cos \delta \cos(\alpha - \phi_r), \quad (16)$$

$$B = \frac{\omega_0 r_E}{c} \cos \delta \sin(\alpha - \phi_r), \quad (17)$$

where ω_0 is the angular frequency of the gravitational-wave signal and r_E is the radius of the Earth. The parameters p , p_0 , and p_1 contain contributions both from the intrinsic evolution of the gravitational wave source and the modulation of the signal due to the motion of the Earth around the Sun. To calculate the false alarm probabilities and determine the grid of templates in the parameter space to do the search for signals in the noise of the detector we introduce yet another approximation to the signal namely we neglect the amplitude modulation and use a signal with a constant amplitude:

$$h(t) = h_0 \sin[\Psi_s(t)], \quad (18)$$

where Ψ_s is the approximate phase given above.

2.2 Optimal data analysis method

We assume that the noise n in the detector is an additive, stationary, Gaussian, and zero-mean random process. Then the data x (if the signal h is present) can be written as

$$x(t) = n(t) + h(t). \quad (19)$$

The log likelihood function has the form

$$\log \Lambda = (x|h) - \frac{1}{2}(h|h), \quad (20)$$

where the scalar product $(\cdot|\cdot)$ is defined by

$$(x|y) := 4 \Re \int_0^\infty \frac{\tilde{x}(f)\tilde{y}^*(f)}{S_h(f)} df. \quad (21)$$

In Eq. (21) \Re means real part, tilde denotes Fourier transform, asterisk is complex conjugation, and S_h is the *one-sided* spectral density of the detector's noise. Assuming that over the bandwidth of the signal h the spectral density $S_h(f)$ is nearly constant and equal to $S_h(f_0)$, where f_0 is the frequency of the signal measured at the SSB at $t = 0$, the log likelihood ratio from Eq. (20) can be approximated by

$$\ln \Lambda \approx \frac{2T_o}{S_h(f_0)} \left(\langle xh \rangle - \frac{1}{2} \langle h^2 \rangle \right). \quad (22)$$

where

$$\langle x \rangle := \frac{1}{T_o} \int_0^{T_o} x(t) dt. \quad (23)$$

The signal h depends linearly on four amplitudes A_i . The likelihood equations for the ML estimators \hat{A}_i of the amplitudes A_i are given by

$$\frac{\partial \ln \Lambda}{\partial A_i} = 0, \quad i = 1, \dots, 4. \quad (24)$$

One can easily find the explicit analytic solution to Eqs. (24). To simplify formulas we assume that *the observation time T_o is an integer multiple of one sidereal day*, i.e., $T_o = n(2\pi/\Omega_r)$ for some positive integer n . Then the time average of the product of the functions a and b vanishes, $\langle ab \rangle = 0$, and the analytic formulas for the ML estimators of the amplitudes are given by

$$\hat{A}_1 \approx 2 \frac{\langle xh_1 \rangle}{\langle a^2 \rangle},$$

$$\hat{A}_2 \approx 2 \frac{\langle xh_2 \rangle}{\langle b^2 \rangle},$$

$$\begin{aligned}\hat{A}_3 &\approx 2 \frac{\langle xh_3 \rangle}{\langle a^2 \rangle}, \\ \hat{A}_4 &\approx 2 \frac{\langle xh_4 \rangle}{\langle b^2 \rangle}.\end{aligned}\tag{25}$$

where

$$\begin{aligned}\langle a^2 \rangle \Big|_{T_o=n \ 2\pi/\Omega_r} &= \frac{1}{4} (1 - 3 \sin^2 \gamma \cos^2 \phi)^2 \cos^4 \delta + \frac{1}{2} \sin^2 \gamma \cos^2 \phi (1 - \sin^2 \gamma \cos^2 \phi) \sin^2 2\delta \\ &\quad + \frac{1}{8} \left[\sin^2 2\gamma \sin^2 \phi + (\cos^2 \gamma - \sin^2 \gamma \sin^2 \phi)^2 \right] (1 + \sin^2 \delta)^2,\end{aligned}\tag{26}$$

$$\begin{aligned}\langle b^2 \rangle \Big|_{T_o=n \ 2\pi/\Omega_r} &= \frac{1}{2} (\sin^2 2\gamma \cos^2 \phi + \sin^4 \gamma \sin^2 2\phi) \cos^2 \delta \\ &\quad + \frac{1}{2} \left(\cos^4 \gamma + \frac{1}{2} \sin^2 2\gamma \sin^2 \phi + \sin^4 \gamma \sin^4 \phi \right) \sin^2 \delta.\end{aligned}\tag{27}$$

The reduced log likelihood function \mathcal{F} is the log likelihood function where amplitude parameters A_i were replaced by their estimators \hat{A}_i . By virtue of Eqs. (25) from Eq. (22) one gets

$$\mathcal{F} \approx \frac{2}{S_h(f_0)T_o} \left(\frac{|F_a|^2}{\langle a^2 \rangle} + \frac{|F_b|^2}{\langle b^2 \rangle} \right),\tag{28}$$

where

$$F_a := \int_0^{T_o} x(t) a(t) \exp[-i\Phi(t)] dt,\tag{29}$$

$$F_b := \int_0^{T_o} x(t) b(t) \exp[-i\Phi(t)] dt.\tag{30}$$

The ML estimators of the signal parameters are obtained in two steps. Firstly, the estimators of the frequency, the spin down parameters, and the angles α and δ are obtained by maximizing the functional \mathcal{F} with respect to these parameters. Secondly, the estimators of the amplitudes A_i are calculated from the analytic formulas (25) with the correlations $\langle xh_i \rangle$ evaluated for the values of the parameters obtained in the first step. Thus filtering for the narrow-band gravitational-wave signal requires *two linear complex* filters. The amplitudes A_i of the signal depend on the physical mechanisms generating gravitational waves. If we know these mechanisms and consequently we know the dependence of A_i on a number of parameters we can estimate these parameters from the estimators of the amplitudes by least-squares method.

We shall next summarize the statistical properties of the functional \mathcal{F} . We first assume that the phase parameters are known and consequently that \mathcal{F} is only a function of random data x (the case when the phase parameters are unknown and need to be estimated will be considered later in this section). When the signal is absent $2\mathcal{F}$ has a χ^2 distribution with four degrees of freedom and when the signal is present it has a noncentral χ^2 distribution with four degrees of freedom and noncentrality parameter equal to the *optimal signal-to-noise ratio* d defined as

$$d := \sqrt{\langle h|h \rangle}. \quad (31)$$

Consequently the probability density functions p_0 and p_1 when respectively the signal is absent and present are given by

$$p_0(\mathcal{F}) = \mathcal{F} \exp(-\mathcal{F}), \quad (32)$$

$$p_1(d, \mathcal{F}) = \frac{\sqrt{2\mathcal{F}}}{d} I_1(d\sqrt{2\mathcal{F}}) \exp\left(-\mathcal{F} - \frac{1}{2}d^2\right), \quad (33)$$

where I_1 is the modified Bessel function of the first kind and order 1. The false alarm probability P_F is the probability that \mathcal{F} exceeds a certain threshold \mathcal{F}_o when there is no signal. In our case we have

$$P_F(\mathcal{F}_o) := \int_{\mathcal{F}_o}^{\infty} p_0(\mathcal{F}) d\mathcal{F} = (1 + \mathcal{F}_o) \exp(-\mathcal{F}_o). \quad (34)$$

The probability of detection P_D is the probability that \mathcal{F} exceeds the threshold \mathcal{F}_o when the signal-to-noise ratio is equal to d :

$$P_D(d, \mathcal{F}_o) := \int_{\mathcal{F}_o}^{\infty} p_1(d, \mathcal{F}) d\mathcal{F}. \quad (35)$$

The integral in the above formula cannot be evaluated in terms of known special functions. We see that when the noise in the detector is Gaussian and the phase parameters are known the probability of detection of the signal depends on a single quantity: the optimal signal-to-noise ratio d . When the phase parameters are unknown the optimal statistics \mathcal{F} depends not only on the random data x but also on the phase parameters that we shall denote by $\boldsymbol{\xi}$. Such an object is called in the theory of stochastic processes a *random field*. Let us consider the correlation function of the random field

$$C(\boldsymbol{\xi}, \boldsymbol{\xi}') := E \{ [\mathcal{F}(\boldsymbol{\xi}) - m(\boldsymbol{\xi})][\mathcal{F}(\boldsymbol{\xi}') - m(\boldsymbol{\xi}')] \}, \quad (36)$$

where

$$m(\boldsymbol{\xi}) := E \{ \mathcal{F}(\boldsymbol{\xi}) \}. \quad (37)$$

For the case of constant amplitude, linear phase model presented in the previous subsection we have

$$m = 1; \quad (38)$$

and

$$\begin{aligned} C(\boldsymbol{\xi}, \boldsymbol{\xi}') = C(\boldsymbol{\xi} - \boldsymbol{\xi}') = & \quad (39) \\ & \langle \cos[\Delta p_0 t + \Delta p_1 t^2 + \Delta A \cos(\Omega_r t) + \Delta B \sin(\Omega_r t)] \rangle^2 + \\ & \langle \sin[\Delta p_0 t + \Delta p_1 t^2 + \Delta A \cos(\Omega_r t) + \Delta B \sin(\Omega_r t)] \rangle^2, \end{aligned}$$

where Δ denotes difference between the parameter values. Thus the correlation function C depends only on the difference $\boldsymbol{\xi} - \boldsymbol{\xi}'$ and on the values of the parameters themselves. In this case the random field \mathcal{F} is called a *homogeneous*. For such fields in Ref. [5] we have developed a theory to calculate the false alarm probabilities that we only summarize here. The main idea is to divide the space of the phase parameters $\boldsymbol{\xi}$ into *elementary cells* which boundary is determined by the *characteristic correlation hypersurface* of the random field \mathcal{F} . The correlation hypersurface is defined by the requirement that at this hypersurface the correlation C equals half of the maximum value of C . Assuming that C attains its maximum value when $\boldsymbol{\xi} - \boldsymbol{\xi}' = 0$ the equation of the characteristic correlation hypersurface reads

$$C(\boldsymbol{\tau}) = \frac{1}{2} C(0), \quad (40)$$

where we have introduced $\boldsymbol{\tau} := \boldsymbol{\xi} - \boldsymbol{\xi}'$. Let us expand the left-hand side of Eq. (40) around $\boldsymbol{\tau} = 0$ up to terms of second order in $\boldsymbol{\tau}$. We arrive at the equation

$$\sum_{i,j=1}^M G_{ij} \tau_i \tau_j = 1, \quad (41)$$

where M is the dimension of the parameter space and the matrix G is defined as follows

$$G_{ij} := - \frac{1}{C(0)} \frac{\partial^2 C(\boldsymbol{\tau})}{\partial \tau_i \partial \tau_j} \Big|_{\boldsymbol{\tau}=0}. \quad (42)$$

Equation (41) defines an M -dimensional hyperellipsoid which we take as an approximation to the characteristic correlation hypersurface of our random field and we call the *correlation hyperellipsoid*. This approximation is helpful in establishing upper limit estimates of the number of elementary cells in the parameter space. The M -dimensional Euclidean volume V_{cell} of the hyperellipsoid defined by Eq. (41) equals

$$V_{cell} = \frac{\pi^{M/2}}{\Gamma(M/2 + 1) \sqrt{\det G}}, \quad (43)$$

where Γ denotes the Gamma function.

We estimate the number N_c of elementary cells by dividing the total Euclidean volume V_{total} of the parameter space by the volume V_{cell} of the correlation hyperellipsoid, i.e. we have

$$N_c = \frac{V_{total}}{V_{cell}}. \quad (44)$$

We approximate the probability distribution of $\mathcal{F}(\boldsymbol{\xi})$ in each cell by the probability distribution $p_0(\mathcal{F})$ when the parameters are known [in our case it is given by Eq. (32)]. The values of the statistics \mathcal{F} in each cell can be considered as independent random variables. The probability that \mathcal{F} does not exceed the threshold \mathcal{F}_o in a given cell is $1 - P_F(\mathcal{F}_o)$, where $P_F(\mathcal{F}_o)$ is given by Eq. (34). Consequently the probability that \mathcal{F} does not exceed the threshold \mathcal{F}_o in *all* the N_c cells is $[1 - P_F(\mathcal{F}_o)]^{N_c}$. The probability P_F^T that \mathcal{F} exceeds \mathcal{F}_o in *one or more* cell is thus given by

$$P_F^T(\mathcal{F}_o) = 1 - [1 - P_F(\mathcal{F}_o)]^{N_c}. \quad (45)$$

This is the false alarm probability when the phase parameters are unknown. The expected number of false alarms N_F is given by

$$N_F = N_c P_F(\mathcal{F}_o). \quad (46)$$

By means of Eqs. (34) and (44), Eq. (46) can be rewritten as

$$N_F = \frac{V_{total}}{V_{cell}} (1 + \mathcal{F}_o) \exp(-\mathcal{F}_o). \quad (47)$$

Using Eq. (46) we can express the false alarm probability P_F^T from Eq. (45) in terms of the expected number of false alarms. Using $\lim_{n \rightarrow \infty} (1 + \frac{x}{n})^n = \exp(x)$ we have that for large number $N_c \gg 1$ of cells

$$P_F^T(\mathcal{F}_o) \approx 1 - \exp(-N_F). \quad (48)$$

When the expected number N_F of false alarms is small, $N_F \ll 1$, we have $P_F^T(\mathcal{F}_o) \approx N_F$.

2.3 Grid of templates

We can only calculate the statistics \mathcal{F} on a finite, discrete grid of points. This leads to an unavoidable loss in the signal-to-noise ratio. In this section we shall outline a construction of a grid in the parameter space such that the loss of the signal-to-noise is minimized. The basic quantity to consider is the expectation values of the statistics $E_1[\mathcal{F}]$ when the signal is present. We again use the constant amplitude linear phase model to carry out the construction. We have that

$$E_1[\mathcal{F}(\boldsymbol{\xi}, \boldsymbol{\xi}')] = 1 + \frac{1}{2}C(\tau), \quad (49)$$

where C is the correlation function of the random field introduced above. We choose the grid of templates in such a way that the correlation between any potential signal present in the data and the nearest point of the grid never falls below a certain value. The critical value of the correlation function can be obtained from the following consideration. The statistics \mathcal{F} can be expressed as a Fourier transform where the parameter p_0 corresponds to angular frequency and consequently \mathcal{F} can be calculated using the FFT algorithm. However the FFT gives the values of the statistics on a certain grid of frequencies called Fourier frequencies. These frequencies in normalized units are separated by factor of 2π . Thus when the true frequency falls between the two Fourier frequencies we cannot achieve the theoretical maximum of the optimal statistics \mathcal{F} . The worst case is when the frequency falls half way between the Fourier frequencies. One can easily calculate that in such a case the signal-to-noise ratio is equal only to 0.63 of the optimal one. This value is too small and we need a finer grid. A way to achieve this and still take advantage of the speed of FFT is either to pad the time series with zeros or to use a special interpolation algorithm invented by pulsar astronomers that work in the Fourier domain. Padding the times series with the same number of zeros as there are data points or using the interpolation algorithms give Fourier transform that is twice as fine as Fourier grid of the FFT of the original data. Then in the worst case the the signal-to-noise is 0.90 of the optimal one. To determine the grid we further approximate the correlation function C of Eq.(39) by Taylor expansion around $\boldsymbol{\tau} = 0$. Keeping terms at most quadratic in τ_i one gets

$$C(\boldsymbol{\tau}) \approx 1 - \sum_{i,j} \tilde{\Gamma}_{ij} \tau_i \tau_j, \quad (50)$$

where the matrix $\tilde{\Gamma}$ has the components

$$\tilde{\Gamma}_{ij} := \left\langle \frac{\partial \Phi}{\partial \tau_i} \frac{\partial \Phi}{\partial \tau_j} \right\rangle - \left\langle \frac{\partial \Phi}{\partial \tau_i} \right\rangle \left\langle \frac{\partial \Phi}{\partial \tau_j} \right\rangle. \quad (51)$$

The matrix $\tilde{\Gamma}$ is the reduced Fisher information matrix. For the linear model given by Eq.(18) the components of the Fisher matrix are constant and Eq.(50) is an equation of the hyperellipsoid. The grid consists of elements that are 4-dimensional prisms inscribed in the ellipsoid given by equation (51) subject to the constraint that frequencies are calculated on a grid that is twice as fine as the Fourier grid. The elementary cell of the grid is a 4-dimensional prism which bases are the two adjacent 3-dimensional hexagonal prisms lying in the planes defined by $\bar{p}_0 = \text{const}$ and separated by $\Delta \bar{p}_0 = \pi$. The details of the construction are given in Ref. ([4]).

3 An all-sky search of the EXPLORER data

We have implemented the theoretical tools presented in the previous Section in the computer codes and we have performed an all-sky search for continuous sources of gravitational waves in the data of the resonant bar detector EXPLORER¹ [2]. This detector has collected many years of data with a high duty cycle (e.g. in 1991 the duty cycle was 75%). The EXPLORER detector was most sensitive over certain two narrow bandwidths (called minus and plus modes) of about 1 Hz wide at two frequencies around 1 kHz. To make the search computationally manageable we analyzed two days of data in the narrow band where the detector had the best sensitivity. By narrowing the bandwidth of the search we can shorten the length of the data to be analyzed as we need to sample the data at only twice the bandwidth. For the sake of the FFT algorithm it is best to keep the length of the data to be a power of 2. Consequently we have chosen the number of data points to analyze to be $N = 2^{18}$. Thus for $T_o = 2$ days of observation time the bandwidth $\Delta\nu$ of the data was $\Delta\nu = N/(2T_o) \sim 0.76$ Hz. We have also chosen to analyze the data for the plus mode which has frequency around 922 Hz. We have used the filters with the phase linear in the parameters, derived in Section 2.1.2. In the filters we have included the amplitude modulation. The number of cells N_c calculated from Eq. (44) was around 1.6×10^{12} . Consequently from Eq. (45) the threshold signal-to-noise ratio for 1% false alarm probability was equal to 8.3. In the search that we have performed we have used a lower threshold signal-to-noise of 6.7. The aim of lowering the threshold is twofold. Firstly the filter we use is only approximately matched the true signal what means that we are losing some signal-to-noise ratio. By lowering the threshold we can catch potential signals that could be lost. Secondly by lowering the threshold we have more candidates from which we can pick up signals by more accurate filtering. We have spaced our templates on the grid derived in Section 2.3. The number of points in the grid over which we had to calculate the statistics \mathcal{F} turned out to be 183064440. This number involved 63830 positions in the sky and 2868 spin down values for each sky position. We have carried out the search on a network of PCs and workstations. We had around two dozens of processors at our disposal. The data analysis took 15 months to complete.

The two-day stretch of data that we analyzed was taken from a larger set of 13 days of data taken by EXPLORER detector in November 1991. We have chosen the 2-day stretch of data on the basis of conformity of the data to the Gaussian random process. We have divided the data into 2^{16} points sections corresponding to around 11 hours of data. For each stretch we have performed the Kolmogorov-Smirnov test and two tests based on the bispectra of the data.

¹The EXPLORER detector is operated by the ROG collaboration located in Italian Istituto Nazionale di Fisica Nucleare (INFN); see <http://www.roma1.infn.it/rog/explorer/explorer.html>.

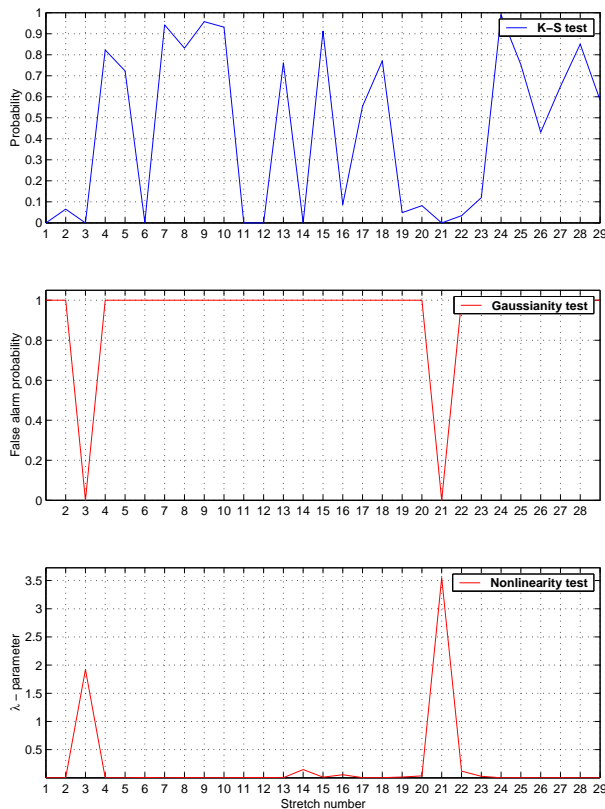


Figure 1: Quality of the EXPLORER data

The Kolmogorov-Smirnov test is well known. One calculates the Kolmogorov-Smirnov distance between the sample distribution and the Gaussian distribution and test the null hypothesis that the data come from the Gaussian distribution. The tests based on the bispectra of the data are explained in the Appendix. The results of the $K - S$ test and the bispectra tests are presented in Figure 1. For the case of $K - S$ test the higher the probability the more Gaussian the data are. For the Gaussianity test low false alarm probability means that non-Gaussianities are present in the data with a high probability. Test for non-linearity is only meaningful when data are non-Gaussian. The value of the λ -parameter indicates the level on non-linearity present in the data. We have also calculated the so-called box plots of the data that display the amount of outliers present. The box and whisker plots for each stretch of data are drawn in Figure 2. Each box has lines at the lower quartile, median, and upper

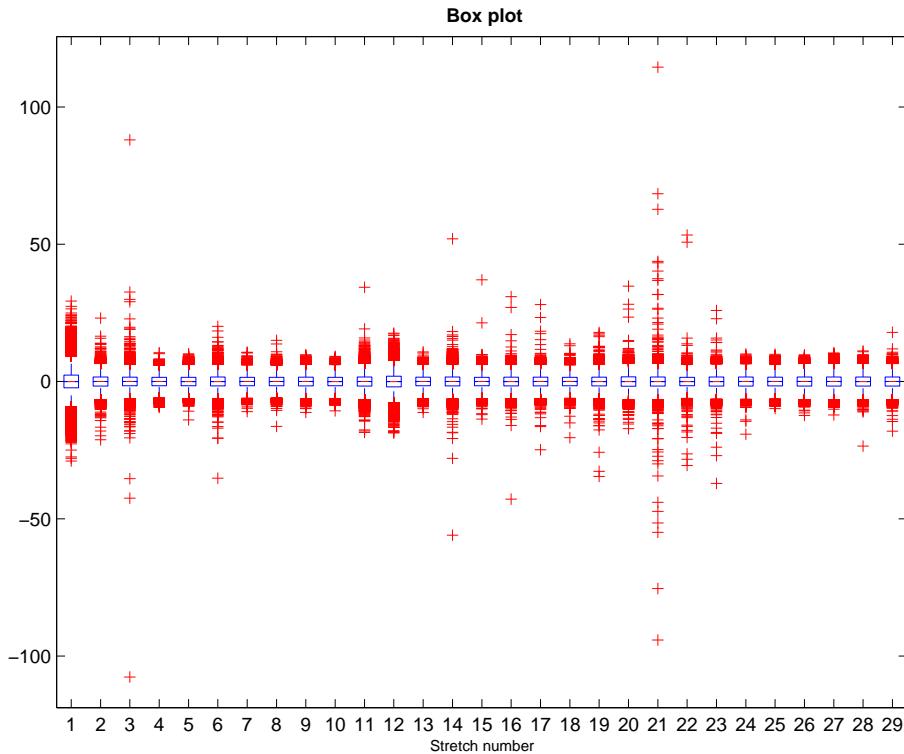


Figure 2: Boxplots of the EXPLORER data

quartile values of the data stretch. The whiskers are lines extending from each end of the box to show the extent of the rest of the data. Outliers are data with values beyond the ends of the whiskers. The whisker extends to the most extreme data value within 1.5 interquartile range of the box. From the above tests we conclude that large parts of data are approximately Gaussian. We also see that whenever a non-Gaussianity is detected the data are also non-linear and moreover the level of outliers is high. On the basis of the above analysis we have chosen the two day data stretch to begin at the first sample of the 7th data stretch. In Figure 3 we have presented the spectral density of the two day stretch of data that we analyzed. We see that minimum spectral density was around $10^{-21}/\sqrt{Hz}$ which was still competitive in comparison to other gravitational-wave detector data available.

We have obtained the 22295 threshold crossings for the Northern Hemisphere and 44701 for the Southern Hemisphere. Not all of these candidates can be considered independent. Candidates that are contained within one cell of the parameter space we

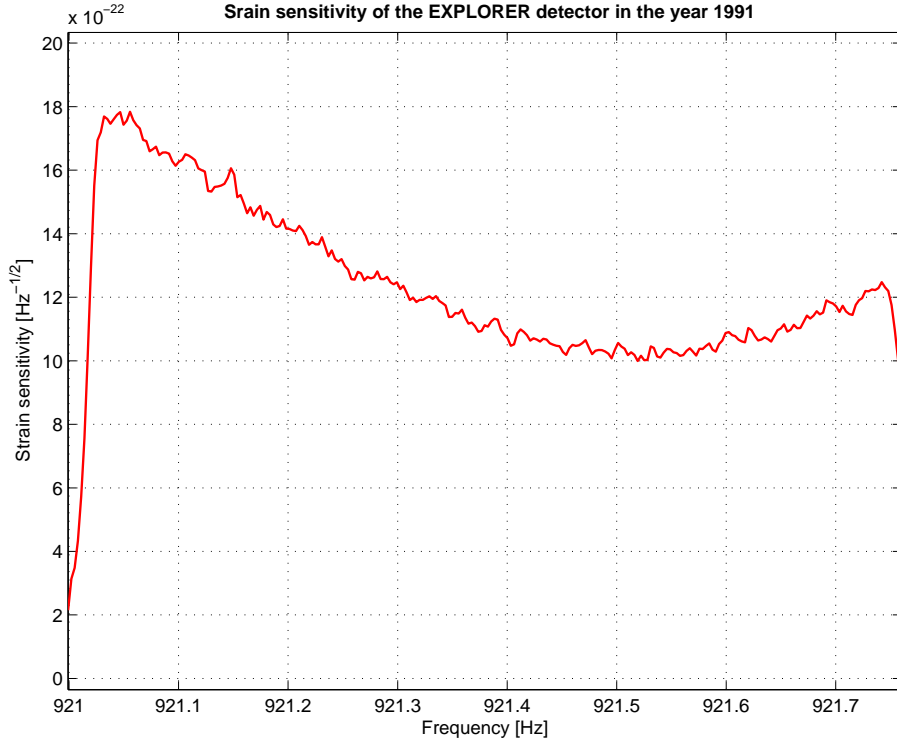


Figure 3: Two-sided spectral density of the EXPLORER data

consider as dependent. Consequently we have obtained 11703 independent candidates for the Northern Hemisphere and 18702 for the Southern Hemisphere. In Figures 4 and 5 we have plotted the histograms of the values of the statistics \mathcal{F} and we have compared it with the theoretical distribution for \mathcal{F} when no signal is present in the data. A good agreement with the theoretical distribution is another indication of Gaussianity of the data. It also reveals that there are no obvious populations of the continuous gravitational wave sources at the level of sensitivity of our search. In the search no event has crossed our 99% confidence threshold of 8.3. The strongest signal had the signal-to-noise ratio of 7.9. The final step of our analysis is the verification of the events using filters based on the accurate model of the signal presented in the previous section. The verification procedure consisted of 4 steps.

1. *Fine search using the linear filter.*
2. *Fine search with accurate templates that includes precise detector ephemeris.*

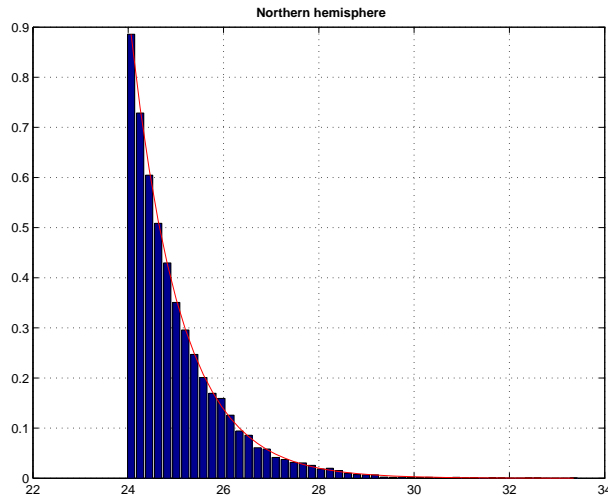


Figure 4: Histogram of candidates: northern hemisphere

3. *Fine search for the signal in a different 2-day stretch of data.*
4. *Fine search of a 4-day stretch of data including the original one.*

The results of the verification procedure for the strongest signal are presented in Figure 6. Since the candidate has not occurred in a different stretch of data than the original one and the signal-to-noise ratio did not increase substantially for twice the original observation time, we conclude that this is not a true gravitational wave candidate. At the moment we have verified only a small fraction of candidates and we cannot yet state a final conclusion of our search. If none of the candidates will be verified i.e. if no true gravitational wave candidate will be found we can make a statement about the upper bound for the gravitational wave amplitude. We take our strongest candidate of signal-to-noise d_o and we suppose that it resulted from a gravitational wave signal. Then, using formula (35), we calculate the signal-to-noise d_{ub} of the gravitational-wave signal so that there is 1% probability that it crosses the threshold corresponding to d_o . The d_{ub} is the desired 99% confidence upper bound. For $d_o = 8.2$, which corresponds to the signal-to-noise ratio of our strongest candidate that we get using the accurate filter (see Figure 6), we find that $d_{ub} = 5.9$. For the EXPLORER detector this corresponds to the dimensionless amplitude of the gravitational wave signal equal to 2×10^{-23} . Thus if no gravitational waves will be found in the search presented above we shall be able to make the following statement:

With 99% confidence the dimensionless amplitude of the gravitational wave signal from a continuous source is less than 2×10^{-23} .

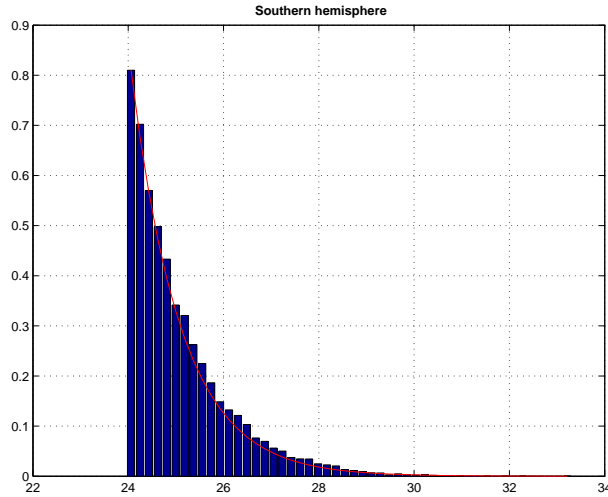


Figure 5: Histogram of candidates: southern hemisphere

A Testing for linearity and Gaussianity using bispectra

We call a process, x_k , linear, if it can be represented by

$$x_k = \sum_l a_l u_{k-l} \quad (52)$$

where u_l is assumed to be independent identically distributed (i.i.d.). If u_l is Gaussian (non-Gaussian), we say that x_l is linear Gaussian (non-Gaussian). In order to test for linearity and Gaussianity we examine the third-order cumulants of the data. We recall that the third order cumulant C_{kl} of a zero mean stationary process is defined by

$$C_{kl} = E[x_m x_{m+k} x_{m+l}]. \quad (53)$$

The bispectrum $S_2(f_1, f_2)$ is the two-dimensional Fourier transform of C_{kl} . The bicoherence is defined as

$$B(f_1, f_2) = \frac{S_2(f_1, f_2)}{S(f_1 + f_2)S(f_1)S(f_2)}, \quad (54)$$

where $S(f)$ is spectral density of the process x_k . If the process is Gaussian then its bispectrum and consequently its bicoherence is zero. One can easily show that if the process is linear then its bicoherence is constant. Thus if the bispectrum is not zero,

then the process is non-Gaussian; if the bicoherence is not constant then the process is also non-linear. Consequently we have the following hypothesis testing problems.

H1: *the bispectrum of x_k is nonzero;*

H0: *the bispectrum of x_k is zero.*

If hypothesis **H1** holds, we can test for linearity, that is, we have a second hypothesis testing problem:

H1': *the bicoherence of x_k is not constant;*

H0': *the bicoherence of x_k is a constant.*

If hypothesis **H0'** holds, the process is linear.

Using the above tests we can *detect* non-Gaussianity and, if the process is non-Gaussian, non-linearity of the process. The distribution of test statistics $B(f_1, f_2)$ (Eq.(54)) can be calculated in terms of χ^2 distributions. For more details see [6].

Acknowledgments

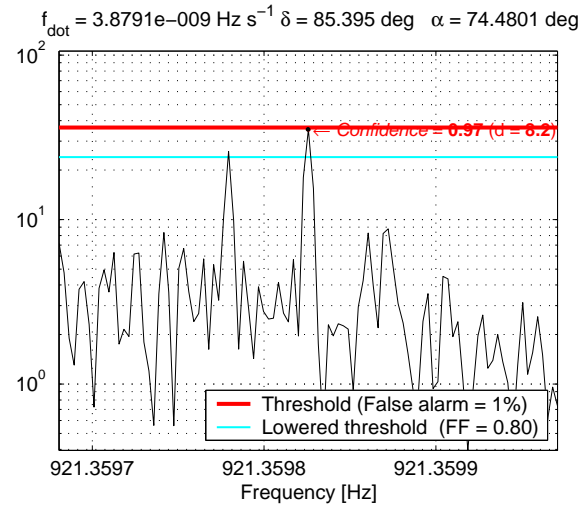
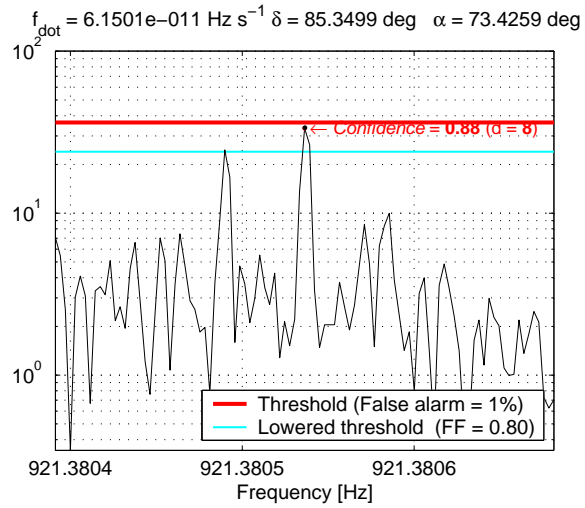
I would like to thank my collaborators Kazik Borkowski, Piotr Jaranowski and members of the *ROG collaboration* for discussions. This work was supported in part by the KBN ([Polish]State Committee for Scientific Research) Grant No. 2P03B 094 17 (A.K.). A part the research described in this paper was performed while the author held an NRC-NASA Resident Research Associateship at the Jet Propulsion Laboratory, California Institute of Technology, under contract with the National Aeronautics and Space Administration. I would also like to thank Interdisciplinary Center for Mathematical and Computational Modeling of Warsaw University for computing time.

References

- [1] P. Jaranowski, A. Królak, and B. F. Schutz, Phys. Rev. D **58**, 063001 (1998).
- [2] P. Astone *et al.*, Phys. Rev. D **47**, 362 (1993).
- [3] P. Astone *et al.*, Phys. Rev. D **65**, 022001 (2002).

- [4] P. Astone, K.M. Borkowski, P. Jaranowski, A. Królak, *Phys. Rev. D* **65**, 042003 (2002)
- [5] P. Jaranowski and A. Królak, *Phys. Rev. D* **61**, 062001 (2000).
- [6] M. J. Hinich, *J. Time Series Analysis* Vol. 3, 169 (1982).

Figure 6: Verification of the candidates



NO SIGNAL FOR DIFFERENT OBSERVATION TIME

